

Journal Pre-proof

A very long-chain fatty acid enzyme gene, PxHacd2 affects the temperature adaptability of a cosmopolitan insect by altering epidermal permeability

Gaoke Lei, Huiling Zhou, Yanting Chen, Liette Vasseur, Geoff M. Gurr, Minsheng You, Shijun You



PII: S0048-9697(23)02993-5

DOI: <https://doi.org/10.1016/j.scitotenv.2023.164372>

Reference: STOTEN 164372

To appear in: *Science of the Total Environment*

Received date: 3 March 2023

Revised date: 4 May 2023

Accepted date: 19 May 2023

Please cite this article as: G. Lei, H. Zhou, Y. Chen, et al., A very long-chain fatty acid enzyme gene, PxHacd2 affects the temperature adaptability of a cosmopolitan insect by altering epidermal permeability, *Science of the Total Environment* (2023), <https://doi.org/10.1016/j.scitotenv.2023.164372>

This is a PDF file of an article that has undergone enhancements after acceptance, such as the addition of a cover page and metadata, and formatting for readability, but it is not yet the definitive version of record. This version will undergo additional copyediting, typesetting and review before it is published in its final form, but we are providing this version to give early visibility of the article. Please note that, during the production process, errors may be discovered which could affect the content, and all legal disclaimers that apply to the journal pertain.

© 2023 Published by Elsevier B.V.

A very long-chain fatty acid enzyme gene, *PxHacd2* affects the temperature adaptability of a cosmopolitan insect by altering epidermal permeability

Gaoke Lei^{a,b,c}, Huiling Zhou^{a,b,c}, Yanting Chen^{a,b,c,d}, Liette Vasseur^{a,b,e}, Geoff M. Gurr^{a,b,f}, Minsheng You^{a,b,c}, and Shijun You^{a,b,c,*}

^a State Key Laboratory for Ecological Pest Control of Fujian and Taiwan Crops, Institute of Applied Ecology, Fujian Agriculture and Forestry University, Fuzhou 350002, China

^b Joint International Research Laboratory of Ecological Pest Control, Ministry of Education, Fuzhou 350002, China

^c Ministerial and Provincial Joint Innovation Centre for Safety Production of Cross-Strait Crops, Fujian Agriculture and Forestry University, Fuzhou 350002, China

^d Institute of Plant Protection, Fujian Academy of Agricultural Sciences, Fuzhou 350013, China

^e Department of Biological Sciences, Brock University, St. Catharines, ON, L2S 3A1, Canada.

^f Gulbali Institute, Charles Sturt University, Orange, NSW, 2800, Australia.

* Corresponding author at: State Key Laboratory for Ecological Pest Control of Fujian and Taiwan Crops, Institute of Applied Ecology, Fujian Agriculture and Forestry University, Fuzhou 350002, China.

E-mail addresses: sjyou@fafu.edu.cn (S. You)

Abstract

Temperature fluctuations pose challenges to poikilotherms, such as insects, especially under climate change conditions. Very long-chain fatty acids (VLCFAs) form important structural components of membranes and epidermal surfaces, so play

important roles in adaptation to temperature stress in plants. It has been unclear whether VLCFAs are involved in epidermis formation and thermal resistance in insects. In this study, we focused on the 3-hydroxy acyl-CoA dehydratase 2 (Hacd2), an important enzyme in the synthesis pathway of VLCFAs, in a cosmopolitan pest, the diamondback moth, *Plutella xylostella*. Hacd2 was cloned from *P. xylostella* and the relative expression pattern was identified. Epidermal permeability increased with the decreased VLCFAs in the Hacd2-deficient *P. xylostella* strain, which was constructed by using the CRISPR/Cas9 system. Survival and fecundity of the Hacd2-deficient strain was significantly lower than that of the wildtype strain when subject to desiccating environmental stress. Hacd2 mediates thermal adaptability in *P. xylostella* by changing epidermal permeability so is likely to be key to it remaining a major pest species under predicted climate change conditions.

Keywords: *Plutella xylostella*; Very long-chain fatty acids; Extreme temperature; CRISPR/Cas9; Water balance

1. Introduction

Global climate change is projected to increase the number of extreme events such as hot and dry episodes (Bauerfeind and Fischer, 2014). Insects and other poikilotherms are highly sensitive to climate variability (Neven, 2000). Extreme temperature environments can easily disrupt their water balance, especially at low humidities. When the ambient temperature exceeds a certain value, transpiration causes insects to rapidly lose water (Gibbs, 2011). The relatively small size of insects limits water storage and increases their surface-to-volume ratio, making them

especially susceptible to transpiration (Krupp et al., 2020). Accordingly, the ability of insects to manage and store water is one of the main factors in their capacity to adapt to wide ranges of environmental conditions and tolerate local extreme events (Beyenbach, 2016). Insects have evolved a series of adaptation mechanisms to maintain their water balance. The insect epidermis is an important barrier to maintaining water balance and internal homeostasis (Balabanidou et al., 2018; Gołębiowski et al., 2008; Roelofs et al., 2009; Vincent and Wegst, 2004; Wang et al., 2016). The upper epidermis and the outer layer of hydrophobic lipids, especially hydrocarbons (CHCs), are mainly involved in this function (Bazin et al., 2010; Chown et al., 2011). Insect's CHCs are also involved in a number of recognition processes (e.g. species recognition, sex recognition, nestmate recognition, recognition of health status, etc.) and alterations in their synthesis could affect not only resistance to dehydration but also recognition and communication (Howard and Blomquist, 2005; van Wigenburg et al., 2010; Beani et al., 2019). Gibbs and Rajpurohit (2010) reports that lipids in the epidermal wax channels dissolve and flow out of the wax channels due to high temperatures, water can penetrate through the voids of wax channels. At the genetic level, the reduced expression of *CYP4G51* in the pea aphid, *Acyrtosiphon pisum* reduces hydrocarbon content and consequently increases mortality under desiccation stress (Chen et al., 2016).

Insect epidermal lipids are complex mixtures of hydrocarbons, alcohols, wax lipids, free fatty acids, triglycerides, etc. (Cerkowniak et al., 2013; Wigglesworth, 1970). Long fatty acid chains and highly saturated fatty acids can increase epidermal

solid-phase lipids and reduce permeability (Gibbs et al., 2003). Generally, fatty acids with more than 20 carbon atoms are defined as VLCFAs (Cassagne et al., 1994; Tvrdik et al., 2000). VLCFAs are directly involved in the composition of the insect epidermis (Cerkowniak et al., 2013; Sutton et al., 2013). They are the main precursors for the synthesis of insect hydrocarbons (Blomquist and Ginzl, 2021; Chung and Carroll, 2015; Ginzl and Blomquist, 2016). The synthesis of VLCFAs is catalyzed by four types of enzymes. First, malonyl-CoA and long-chain acyl-CoA are condensed by fatty acid elongases (ELO) to form very-long-chain 3-oxoacyl-CoA. Second, very-long-chain 3-oxoacyl-CoA is reduced to very-long-chain (3R)-3-hydroxy acyl-CoA and catalyzed by hydroxysteroid 17-beta dehydrogenase (HSD). Third, the substrate is dehydrated by 3-hydroxyacyl-CoA dehydratase (HACD) to form very-long-chain trans-2,3-dehydroacyl-CoA (Bach et al., 2008). Finally, terraced (TER) reduces it to long-chain acyl-CoA (C_{n+2}), which undergoes several cycles to form VLCFAs of different lengths. Notwithstanding this knowledge of synthesis, the functional role of VLCFAs in insects exposed to extreme temperatures has not been well understood.

Studies in plants suggest that VLCFAs are also involved in plant response to temperature extremes. For example, tomato *phingolipid delta8 desaturase* gene knock-out results in the disruption of chloroplast membranes, swelling of thylakoids, and reduced granal stacking in plants exposed to low temperatures. These results show that free Long-Chain Bas (LCB) (one of the VLCFAs) is crucial for chilling resistance in tomato (Zhou et al., 2016). Unsaturated VLCFAs increase by 6% when *Nicotiana tabacum* L. is transferred from 22-24°C to 8°C for 6 days. In low

temperatures, the unsaturation of VLCFAs can improve the cold resistance of plants (Popov et al., 2012). During summer, a significant amount of VLCFAs accumulates in *Polyiphonia lanosa*, the accumulation of saturated membrane fatty acids at higher temperatures prevents membranes from over-fluidisation (Pettitt et al., 1989). Considering the role of VLCFAs and related genes play in plants, it is possible that these effects may also be of relevance in insect temperature adaptation.

Diamondback moth, *Plutella xylostella* (L.) (Lepidoptera: Plutellidae), is a cosmopolitan pest of cruciferous species (Talekar and She ton, 1993), responsible for annual damage and management costs of US \$4-5 billion worldwide (Furlong et al., 2013). It is suspected that *P. xylostella* can adapt to future climates in most parts of the world through high genetic tolerance and thus remaining a serious pest worldwide (Chen et al., 2021; You et al., 2020). It is important to understand insect adaptation mechanisms to extreme temperatures to help guide the development of pest control measures (Kang et al., 2009). The lipid on the surface of an insect's body directly connects the internal and external environments, which is the first line of defense against stress (Beament, 1958). Many of the genes involved in epidermal lipid synthesis may be potential targets for the control of pests such as *P. xylostella*. When the epidermal barrier is compromised, insects are less able to adapt to extreme environments and the likelihood of infiltration by harmful substances such as pesticides and pathogens may increase. For example, when the structure of the cuticle waxy layer is destroyed, its sensitivity to deltamethrin insecticides is increased (Vincent, 2001). RNAi knockout of *LmFAS1* and *LmFAS3* increases water evaporation

and mortality of the locust, *Locusta migratoria* (Yang et al., 2020). However, little is known about the mechanism of lipid synthesis on the surface of the body of *P. xylostella* and its function in temperature adaptation.

Of the four proteins involved in the synthesis of VLCFAs, ELO has been the most well studied. It has been shown that ELO is involved in fatty acid synthesis and epidermal composition in insects (Danielsen et al., 2016; Zhao et al., 2020). The potential function of the other three proteins, however, is unclear. In this study, a bioinformatics analysis of the *Hacd2* in *P. xylostella* was performed. The expression levels of *PxHacd2* were detected at different temperatures to determine its possible function in temperature adaptation. The *PxHacd2* gene was analysed for spatiotemporal expression to determine whether *PxHacd2* has an important function in certain developmental stages or tissues. In this work, the mutant *PxHacd2* line was generated by the CRISPR/Cas9 technology. We determined the total VLCFAs concentration in wild-type and mutant at different developmental stages. Our results suggested that *PxHacd2* was involved in the synthesis of VLCFAs. The involvement of *PxHacd2* in maintaining a water balance in *P. xylostella* was demonstrated by Eosin Y staining, and by counting the survival of the wild type and mutants at different humidity environments. We further used the age-stage-specific sex life tables of each strain to elucidate how those changes in the epidermal permeability of *P. xylostella* might affect its development and reproduction at different temperatures. Finally, the adaptation mechanism of *PxHacd2* to temperature changes by altering the epidermal permeability of *P. xylostella* was determined by performing the high-temperature

stress treatment at 42°C and by detecting the overcooling point and freezing point of pupae. Our results confirmed the crucial roles of *PxHacd2* in maintaining epidermal permeability of *P. xylostella*, suggesting that this gene might be potential targets for pest control.

2. Materials and methods

2.1. Insect strains

The wild strain of *P. xylostella* was donated by the Institute of Zoology, Chinese Academy of Sciences, in 2015. It was maintained in a climate chamber with the following conditions: photoperiod of 12 L:12 D, $26\pm 0.5^\circ\text{C}$, and $60\%\pm 5\%$ relative humidity. The larvae were reared in sterile plastic disposable 90 mm petri dishes on an artificial diet containing 68 g yeast powder, 20.4 g agar, 127.5 g raw wheat germ, 3.4 g potassium sorbate, 3.4 g methyl paraben, 34 g sucrose, 10.2 g powder of radish seed, 1.7 g vitamin premix, 3.4 g ascorbic acid, 3.4 mL cola oil, 0.34 mL linoleic acid and 850 mL water. Adults were transferred into disposable paper cups (10.8 cm deep, 8.2 cm upper inside diameter, and 5.2 cm lower inside diameter) for mating and oviposition. A 10% honey solution was also provided (Huang et al., 2017).

2.2. Gene cloning

To obtain a correct gene model, full-length cDNA was amplified and sequenced. Five 4th instar larvae were collected and combined to extract total RNA using the Eastep® Super Total 105 RNA Extraction Kit (Promega, USA). RNA was quantified by Nanodrop 2000 spectrophotometer (GE-Healthcare, USA) and checked for integrity by agarose gel electrophoresis (1%) (Xie et al., 2020). cDNA template was obtained

using the Reverse-Transcription System Kit (Promega, USA), with the following processing steps. The reaction mixture A contained RNA (2000 ng), Random primer (1.0 μ L), Oligo primer (1.0 μ L), and nuclease-free water to make up 10 μ L total volume. The reaction mixture A was incubated for 5 min at 70°C. Then, the reaction mixture B containing 4.0 μ L GoScript 5 \times Reaction Buffer, 2.0 μ L 25 mM MgCl₂, 1.0 μ L PCR Nucleotide Mix, 0.4 μ L Ribonuclease inhibitor, 1.0 μ L GoScript Reverse Transcriptase (RT) and 1.0 μ L Nuclease-free water was added to the reaction mixture A to form reaction mixture C. The reaction mixture C was incubated for 5 min at 25 °C, 60 min at 42 °C, and 15 min at 70 °C. The resulting cDNA was stored at -20 °C (Ji et al., 2015).

The reference sequences of *PxHacd2* were obtained from DBM genome-sequencing databases (<http://iae.fafu.edu.cn/DBM/index.php>). Primers for the full length of exons (primer: *PxHacd2*-CDS-F; *PxHacd2*-CDS-R) were designed using Primer Premier 6.0 software. The amplification primers are listed in Table 1. The 4th instar larval cDNA was used as the template and PCR amplification of *PxHacd2* employing the Phanta[®] Max Super-Fidelity DNA Polymerase (Vazyme, Nanjing, China). The 50- μ L PCR reaction mixture was 2 \times Reaction Buffer (25.0 μ L), dNTP Mix (1.0 μ L), 20 μ M F primer (2.0 μ L); 20 μ M R primer (2.0 μ L), DNA polymerase (1.0 μ L), nuclease-free water (15 μ L) and cDNA (4.0 μ L). The amplification program was as follows: 95°C for 3 min, followed by 34 cycles at 95°C for 15 s, 58°C for 15 s, 72°C for 40 s, and 72°C for 5 min (Xu et al., 2022). The PCR products were verified by 2% agarose gel electrophoresis. The PCR fragment was

purified using the gel extraction kit (Omega, USA) (Jiang et al., 2022) and ligated into a pESI-Blunt simple vector (YEASEN, Shanghai) (Xie et al., 2022). The ligated product was transferred into DH5 α -competent cells and spread on LB+100 μ g/ml Ampicillin plates, incubated overnight at 37°C. A single colony was picked and placed in 500 μ L of liquid LB medium with 100 μ g/mL of ampicillin (Zhou et al., 2022). A positive clone was sent to Tsingke Biotechnology Inc (Beijing, China) for sequencing.

2.3. Sequence analysis and phylogenetic tree construction

In order to obtain comprehensive gene function information, the following experiments were carried out. The cDNA sequence of the *PxHacd2* obtained by cloning was compared with the full-length cDNA of the gene from the DBM-genome database (<http://iae.fafu.edu.cn/DBM/index.php>). Conserved domains and protein-coding sequences of *PxHacd2* were predicted by using NCBI (<https://blast.ncbi.nlm.nih.gov/Blast.cgi>). Predictions of *PxHacd2* relative molecular mass and isoelectric point were obtained by using the proteome prediction tool ExPASy (<http://expasy.org/tools/dna.html>). Protein secondary structures and transmembrane regions were predicted using PSIPRED (<http://bioinf.cs.ucl.ac.uk/psipred/>) and TMHMM Server (v.2.0, <http://www.cbs.dtu.dk/services/TMHMM>), respectively. The phylogenetic tree was constructed by using the neighbor-joining (NJ) algorithm and implemented in MEGA7 for 1000 bootstraps (reference) (Zhou et al., 2022).

2.4. Expression profiling of *PxHacd2*

2.4.1. *PxHacd2* expression patterns at different developmental stages and tissues

The expression levels and patterns of *PxHacd2* in *P. xylostella* were analyzed in different developmental stages and tissues. Total RNA from developmental stages (eggs, 1-4 instars, pupae, male adults, and female adults) and tissues (head, midgut, epidermis, fat body, Malpighian tube, and silk gland of the 4th instar larvae) were generated using the same method as in 2.2. Three biological replicates and three technical replicates for each biological replicate were used for each stage and tissue sample. The primers used in qRT-PCR assays are described in Table 1 (primers: Q-*PxHacd2*-F; Q-*PxHacd2*-R). The internal reference gene was the *RPL32* gene of the moth (primers: Q-*PxRPL32*-F; Q-*PxRPL32*-R). The qPCR was performed with Taq Pro Universal SYBR qPCR Master Mix (Vazyme, Nanjing, China). The 20- μ L qPCR reaction was a mixture of 2 \times Taq Pro Universal qPCR Master Mix (10 μ L), 20 μ M F primer (0.4 μ L); 20 μ M R primer (0.4 μ L), Nuclease Free Water (7.15 μ L), and cDNA template (2 μ L). The qRT-PCR was conducted using QuantStudio 3 Real-Time PCR System (Thermo, USA). The program was as follows: 95°C for 30 s, followed by 40 cycles at 95°C for 10 s, 60°C for 20 s. The melting curve acquisition was performed at 95°C for 15 s, then 60°C for 1 min, and 95°C for 15 s (Li et al., 2022).

2.4.2. Expression patterns at extreme temperatures

Ten 3rd instar larvae were transferred into a 60-mm petri dish. Three petri dishes with 10 individuals each were then exposed to one of the following temperatures for 2 hours: 12°C, 10°C, 8°C, 6°C, 4°C, 32°C, 34°C, 36°C, 38°C and 40°C. After exposure, all samples were immediately frozen in liquid nitrogen for 10 min and stored at -80°C for RNA extraction. The RNA extraction, reverse transcription, and qRT-PCR methods

were the same as in 2.4.1.

2.5. *PxHacd2* gene deletion using CRISPR/Cas9 genome editing

2.5.1. Screening sgRNA target

To verify the function of *PxHacd2*, we constructed a homozygous mutant *P. xylostella* line of the *PxHacd2* gene using CRISPR/Cas9 system. Target design was based on the 5'-N20NGG-3' (the PAM sequence is underlined) principle, with potential off-target effects of sgRNA, predicted using Cas-OFFinder (<http://www.rgenome.net/cas-offinder>) (Xie et al., 2019). One sgRNA recognition site was screened in exon 3. The forward primer contained the T7 promoter sequence, target, and sgRNA scaffold sequence, and the antisense primer contained a partial sgRNA sequence that was complementary to the forward primer sgRNA scaffold sequence (Zou et al., 2020).

2.5.2. sgRNA synthesis and purification

The in-vitro transcription template for sgRNA was generated from a single nucleotide strand (*PxHacd2*-SgRNA-F; sgRNA-Com-R) (Table 1) under the following reaction conditions: 95°C for 3 min, followed by 30 cycles at 95°C for 15 s, 68°C for 15 s, 72°C for 30 s, and 72°C for 5 min. The product was excised and recovered by gel extraction using the same method as in 2.2. The sgRNA was obtained by in vitro transcription of the gel product using the HiScribe™ T7 Quick High Yield RNA Synthesis Kit (New England Biolabs, USA). The sgRNA was purified using phenol:chloroform extraction. The method for determining the concentration and quality of the product was the same as 2.2. (Hwang et al., 2013).

2.5.3. sgRNA/Cas9 protein microinjection

Microinjection solutions contained 300 ng/ μ L of sgRNA, 200 ng/ μ L of Cas9 protein (GenCrispr, Nanjing, China), 1 μ L of 10 \times Reaction Buffer, made up to 10 μ L with nuclease-free water, and incubate at 37 °C for 25 min. The mixture was injected into newly laid eggs using an Olympus SZX16 microinjection system (Olympus, Japan), the whole microinjection was completed within 30 minutes. The female adults laid their eggs on an egg card with indentations (a parafilm coated with turnip seed powder). One egg card contained approximately 50 eggs and two cards were used for injection. Each microinjected egg card was transferred into a 90 mm petri dish to hatch. The hatched eggs were fed under the same conditions as 2.1. and any hatched or dead eggs were noted.

2.6. Mutation screening

To detect CRISPR/Cas9-induced mutations, PCR amplification and sequencing were performed using specific primers (primers: *PxHacd2-F*; *PxHacd2-R*) (Table 1). Genomic DNA was extracted from adults using the TiANamp Genomic DNA Kit (TIANGEN, China). The target sequence amplification program was as follows: 95°C for 3 min, followed by 34 cycles at 95°C for 15 s, 58°C for 15 s, 72°C for 15 s, and 72°C for 5 min. The rest of the conditions are the same as described in 2.2. The PCR products were verified by 1% agarose gel electrophoresis, and Sanger sequenced by Tsingke Biotechnology Inc.

The injected eggs were designated as generation 0 (G0). The eggs were reared into adults, crossed with a wild (not injected) adult and used to extract G0 adults

gDNA after laying eggs (these constituting G1 progeny). PCR products flanking the two sgRNA target sites were amplified as indicated above to determine the genotypes and select lines to retain (i.e., individuals whose sequence chromatograms contained double peaks in the nucleotide positions starting at the sgRNA target site). G1 eggs were reared to the adult life stage and these G1 moths were sibling mated to generate G2 progeny. All G1 adults were then individually identified by PCR-based genotyping. G2 produced by heterozygous G1 with the same allelic mutation were collected and sibling crossed to obtain the G3 progeny. The G3 progeny with homozygous mutations was kept, and mass crossed to establish homozygous strain. If heterozygotes were obtained, in-crossing continued until homozygous mutations were generated.

2.7. Determination of very-long-chain fatty acids

To investigate whether knock-out of *PxHacd2* in *P. xylostella* had an effect on the VLCFAs concentration, we measured VLCFAs in 4th instar larvae, pupae, and adult males and females of wild and mutant strains using the VLCFAs assay kit (Shanghai Zcibio Technology Co., Ltd, China). Components of the kit included: Different concentrations of the standard (500 pg/mL, 250 pg/mL, 125 pg/mL, 62.5 pg/mL, 31.25 pg/mL and 0 pg/mL); microtiter plate wells coated with VLCFAs antibody; an antigen labeled with horseradish peroxidase (HRP); reaction solution A (0.01% hydrogen peroxide); reaction solution B (0.1% 3,3',5,5'-tetramethylbenzidine); stop solution (2 mol/L sulfuric acid); and wash buffer (1X) (0.0025% Tween-20). Before starting the measurement, all reagents were conditioned to room temperature. The

reaction solution C was prepared according to the ratio of reaction solution A: reaction solution B = 1 : 1 (v : v). A sample of 50 mg was put into a 1.5 mL centrifuge tube with 500 μ L pre-chilled phosphate buffered saline. The sample was fully ground then centrifuged at 4°C, 5000 \times g for 10 min and the supernatant transferred into a new tube. The subsequent method was as follows: addition of 50 μ L standard or sample into microtiter well, and then addition of 100 μ L HRP. After an incubation for 60 min at 37°C, the plate was washed 5 times with wash buffer (1 \times). Then, 100 μ L of solution C was added into each well and incubated for 15 min at 37 °C. Once completed, 50 μ L of stop solution was added and the OD value at 450 nm was measured with a microplate reader. The OD value was negatively correlated with the concentration of VLCFAs. A fitted curve was prepared using a range of various standard concentrations. The standard curve was performed using the 4-parameter logistic: $y = (2.57654 - 0.16451) / (1 + (x / 19.23495) \times 2.0293) + 0.16451$, $r^2=0.99931$, and this allowed the concentration of VLCFAs in the samples to be calculated (Engvall and Perlmann, 1971)

2.8. Eosin Y staining

We did the following experiments to investigate whether knockout of *PxHacd2* affected the epidermal permeability of the moth. The 4th instar larvae of wild-type and mutant moths were immersed in a 2.0 ml tube filled, which contained 1.5 ml of 0.5% (weight/volume) Eosin Y solution and stained for 2 h in a 45°C water bath. Insects were then washed with ddH₂O until the excess dye was removed. Finally, a light microscope (Leica DMI8, magnification \times 3.0) was used to observe and

photograph the epidermis of the moths (Yang et al., 2020).

2.9. Water retention test

To study the effect of the *PxHacd2* gene on water retention forty newly-emerged adults of the wild type (twenty females, twenty males) or mutant moths (twenty females, twenty males) were put into hermetically sealed transparent boxes (32 cm × 22 cm × 10 cm) with different humidity levels. The drying box contained 500 mg silica gel desiccant to simulate a dry environment (humidity drops when the box was sealed), and the high-humidity box contained the same volume of water to simulate a high humidity environment (humidity rises when the box was sealed). The boxes are externally sealed with parafilm. The boxes were then placed in the same environment as 2.1. The level of humidity was measured with a hygrometer (TRSI, China). The relative humidity in the drying box decreased from the initial humidity (a relative humidity of about 60%) to below 10% in the first 15 minutes. The relative humidity in a high humidity box was initial humidity at the start and up to over 90% in the first 15 minutes. The control experiments were performed using the same volume of plastic pellets (about 2mm in diameter) (Before the tests and for the removal of the moisture from plastic pellets, they were dried in an oven for 3 days at 60 °C) instead of desiccant or water. The material (desiccant/water/plastic pellets) was replaced in the boxes every 24 h leaving the air in the boxes to be replenished. The number of surviving moths was recorded daily until all adults died. Each treatment was repeated 4 times (total of 160 wild and 160 mutant individuals) (Yang et al., 2020).

2.10. Age-stage-specific sex life table

To investigate the effect of knocking out *PxHacd2* gene on the acclimatization of *P. xylostella* at different temperature environments, we constructed life tables of wild and mutant strains at different temperature environments. Life tables for both wild and mutant strains were developed by exposing 120 newly laid eggs (<30 min) of each strain to one of the following temperatures: normal temperature (26°C), high temperature (12h:12h=32°C:27°C), or low temperature (12h:12h=15°C:10°C). The other environmental conditions were the same as in Section 2.1. The eggs from each strain were individually transferred into a 30 mm Petri dish and fed with the same artificial diets as previously described (food replaced every two days). The survival and the time until the pupation of a single moth was recorded. At the pupal stage, pupae were transferred into a perforated 1.5 mL centrifuge tube. One newly emerged adult female and one newly emerged adult male were placed in a 25 mL plastic cup and provided with a 10% honey solution for mating and oviposition. The number of eggs laid by each female adult was recorded daily until its death. The longevities of both male and female were recorded. Each egg was considered a replicate (Yang et al., 2021).

TWOSEX-MSChar computer program (<http://140.120.197.173/ecology/prod2.htm>) was used to calculate the life history data (Chi, 1988). It calculated the survival rate (S_{xj}), the age-specific survival rate (l_x), the age-specific fecundity (m_x), the age-stage-specific fecundity (f_{xj}), the mean generation time (T), the intrinsic rate of increase (r), the finite rate of increase (λ),

and the net reproductive rate (R_0). The formulae were as follows:

$$l_x = \sum_{j=1}^m s_{xj}$$

$$m_x = \frac{\sum_{j=1}^m s_{xj} f_{xj}}{\sum_{j=1}^m s_{xj}}$$

$$R_0 = \sum_{x=0}^{\infty} l_x m_x$$

$$\sum_{x=0}^{\infty} e^{-r(x+1)} l_x m_x = 1$$

$$\lambda = e^r$$

$$T = (\ln R_0) / r$$

The standard errors of population parameters were subjected to 100,000 re-samplings using the bootstrap method (Ebrahimi et al., 2013). Plots were made using SigmaPlot 12.0.

2.11. Response to high temperature

To investigate the effect of knocking out *PxHacd2* gene on the moth's ability to respond to extreme heat, we did the following experiments. To obtain enough males and females for the experiment, 1000 pupae of either the wild or mutant strain were placed singly into a perforated 1.5 mL centrifuge tube. Newly emerged adults were collected for the test. Each replicate consisted of either 20 males or 20 females, and 4 replicates of each treatment were carried out. Each individual was exposed to 42°C for one of these exposure times: 30 min, 60 min, 90 min, 120 min, or 150 min (20 males and 20 females x 2 strains (wild and mutant) x 5 treatments x 4 replicates =

1600 tubes). After exposition, the treated moths were placed in an artificial climate box for 24 h at 26°C and the survival rate was recorded. The moth was considered to be alive when it showed any movement of a limb (antennae, feet, and mouthpart) (Zhou et al., 2022).

2.12. Supercooling point and freezing point

We also investigated the effect of knocking out *PxHacd2* gene on the resistance capacity of the moth to low temperatures. Thirty randomly selected 2-day-old pupae of each wild or mutant strain were collected to determine the supercooling point and freezing point. To do so, a thermistor probe of the subcooling point tester (Omega, USA) was taped to a pupa, secured with conductive tape and placed in a centrifuge tube, with the mouth of the tube sealed with cotton. The centrifuge tubes were transferred into an ultra-low temperature refrigerator at -70°C, with the temperature dropping rapidly at the beginning, and then by 0.10°C per second toward the supercooling point. The temperature was recorded up to the supercooling point, which is the temperature at which the insect body fluids freeze and release latent heat or the freezing point when ice is forming inside the pupa (Hao and Kang, 2004).

2.13. Statistical analyses

The relative expression of *PxHacd2* was calculated for each different stage and tissue based on the $2^{-\Delta Ct}$ method (Yeh et al., 2011). The relative expression level of *PxHacd2* at different temperature treatments was calculated by the comparative $2^{-\Delta\Delta CT}$ method (Conley-LaComb et al., 2013). Statistical analysis was performed using SPSS 23.0 (SPSS, USA). The data were tested for normal distribution using the

Shapiro-Wilk method, and differences between wild and mutant strains were analyzed using the independent samples t-test if the data conformed to a normal distribution, or the Mann-Whitney U test for differences if they did not conform to a normal distribution.

3. Results

3.1. Sequence alignment and phylogenetic tree of *PxHacd2*

The *PxHacd2* gene contained four exons and three introns. *PxHacd2* contained one highly conserved domain, which belonged to the superfamily of protein tyrosine phosphatase-like protein (PTPLA) (Figure 1a).

PxHacd2 had an open reading frame of 696 bp and encoded 231 amino acids, which was consistent with the reference sequence of the DBM-genome. *PxHacd2* protein was a hydrophobic protein. The molecular mass and isoelectric point of *PxHacd2* protein were 26311.97Da and 9.35, respectively. The secondary structure of the *PxHacd2* was predicted to be mainly α -helix and random coil (Figure 1b). DeepTMHMM predicted that the *PxHacd2* contained six transmembrane structural domains, indicating that it was a transmembrane protein (Figure 1c).

The phylogenetic tree showed that *PxHacd2* of *P. xylostella* and *Spodoptera frugiperda* were sister clades. *Vanessa tameamea*, *Zerene cesonia*, *Vanessa tameamea*, *Maniola hyperantus*, *Colias croceus*, *Papilio machaon*, and *Papilio polyte*, in turn, formed a separate monophyletic group (Figure 1d).

3.2. Expression level of *PxHacd2* at different developmental stages and in tissues at different temperatures

We examined the *PxHacd2* gene in *P. xylostella* spatiotemporal expression pattern and the effect of temperature changes on its expression. We found that the expression level of *PxHacd2* was highest in the pupae. The relative expression of *PxHacd2* was not significantly different among the other stages, and all were lower than in the pupae (Figure 2a). *PxHacd2* expression was highest in the fat body and epidermis in the 4th instar larvae, with no significant differences among the other tissues (head, midgut, markov tube, sericterium), and all were lower than the fat body and epidermis (Figure 2b). In addition, after 2 h of rearing 3rd instar larvae at different high and low temperatures, we found that the expression of the *PxHacd2* gene was reduced at 32°C ($t=3.584$, $df=4$, $P=0.023$), 34°C ($t=5.496$, $df=4$, $P=0.005$), 36°C ($t=8.337$, $df=4$, $P=0.001$), 38°C ($t=3.142$, $df=4$, $P=0.035$), 40°C ($t=3.053$, $df=4$, $P=0.038$), 12°C ($t=3.411$, $df=4$, $P=0.027$), 10°C ($t=8.565$, $df=4$, $P=0.001$), 8°C ($t=8.914$, $df=4$, $P=0.001$), 6°C ($t=6.93$, $df=4$, $P=0.002$) and 4°C ($t=8.346$, $df=4$, $P=0.001$) compared to that at 26°C (Figure 2c).

3.3. *PxHacd2* pure mutant strain

Of the 100 eggs subject to CRISPR/Cas9 treatment, 56 % successfully developed into adults. Sequencing showed that 3.57 % (2/56) had exon 3 mutations. After mating and egg laying, the G1 generation was sequenced and the mutation type +4/-20 bp was identified. Self-crossing was continued and a +4/-20bp homozygous mutation was obtained in the G4 generation (Figure 3c).

3.4. Content of VLCFAs

The VLCFAs level was significantly reduced in different developmental stages of

the mutant strain as compared with the wild-type strain (4th instar larvae: $t=6.579$, $df=8$, $P<0.001$, pupae: $t=5.452$, $df=8$, $P=0.01$, female adult: $t=5.433$, $df=8$, $P=0.001$, male adult: $t=7.667$, $df=8$, $P<0.001$) (Figure 3a). In addition, the concentration of VLCFAs in the samples was highest in 4th instar larvae compared with other life stages (Figure 3b).

3.5. Eosin Y staining

To investigate the effect of VLCFA synthesis on epidermis inward permeability, Eosin Y staining was performed on wild-type and mutant 4th instar larvae. Compared to the wild-type strain, Eosin Y penetrated the anterior and caudal parts of the mutant strain, becoming red (Figure 3d).

3.6. Water-retention

To investigate the effect of *PxHacd2* on water retention in adult *P. xylostella*, wild-type and mutant strains were placed in different humidity environments. We found that the survival rate of female adults of the mutant strain was significantly lower on days 2 ($t=11.359$, $df=6$, $P<0.001$) and 3 ($Z=-2.381$, $P=0.029$) compared to the wild strain under low humidity conditions (<10%), and the survival rate of male adults of the mutant strain on day 2 ($t=3.19$, $df=6$, $P=0.019$) was significantly lower. Under normal humidity (60±5%), the survival rate of female adults on days 3 ($Z=-2.233$, $P=0.029$), 4 ($t=10.51$, $df=6$, $P<0.001$), 5 ($Z=-2.352$, $P=0.029$) and male adults on days 4 ($Z=-2.381$, $P=0.029$) and 5 ($Z=-2.53$, $P=0.029$) of the mutant strain was significantly lower compared to the wild strain. Under high humidity (>90%), the survival rate of female adults of the mutant strain was significantly reduced on days 4

($Z=-2.381$, $P=0.029$), 5 ($Z=-2.337$, $P=0.029$), 6 ($t=20.221$, $df=6$, $P<0.001$), 7 ($t=28.723$, $df=6$, $P<0.001$) and male adults on days 3 ($Z=-2.233$, $P=0.029$), 4 ($Z=-2.381$, $P=0.029$), 5 ($Z=-2.381$, $P=0.029$), 6 ($Z=-2.352$, $P=0.029$), 7 ($t=7.406$, $df=6$, $P<0.001$). The maximum number of days for the lifespan of male adults of the mutant strain at low humidity, female and male adults of the mutant strain at normal humidity and female and male adults of the mutant strain at high humidity were 3, 6, 5, 7 and 7 days, respectively. These were lower than the maximum survival days of the wild strain in the same environment of 4, 7, 8, 11 and 11 days, respectively (Figure 4).

3.7. Age-stage-specific sex life table

The development time of the larval stage was significantly longer for the mutant strain compared with the wild-type strain under normal, high, or low temperatures (Table 2). The adult lifespan, longevity, fecundity, and oviposition of the mutant strain were significantly lower compared to the wild-type strain under normal, high, or low temperatures, with the exception of the longevity of mutant males at low temperature (Table 2). The intrinsic rate of increase (r) (normal: $P<0.001$, high: $P<0.001$, low: $P<0.001$), net reproductive rate (R_0) (normal: $P<0.001$, high: $P<0.001$, low: $P<0.001$), and finite rate of increase (λ) (normal: $P<0.001$, high: $P<0.001$, low: $P<0.001$) of the mutant population were significantly lower than those of the wild-type strain at different temperatures. The generation time (T) of mutants was significantly longer at normal and low temperatures than the wild type. There was no significant difference in T between the two strains at high temperatures ($P=0.174$) (Table 2).

The survival rate s_{xj} is the probability that a neonate survives to age x and stage j . The survival rates of immature stages (larval and pupal stages) were 80% and 40% for the wild type and the mutant strains, respectively, at normal temperature (26°C). At high temperature (12h:12h=32°C:27°C), the values were 52% for the wild-type and 22% for the mutant, and at low temperature (12h:12h=15°C:10°C), 77% for the wild type and 18% for the mutant (Figure 5i).

The l_x curve, describing the change in the survival rate of the population with age, showed that the mutant strain exhibited a strong decline in survival rate in the immature stage and a short overall lifespan at the same temperature environment compared with the wild-type strain. The f_{xj} curve describes the daily number of eggs produced per female of age x and stage j . The highest daily fecundities of the wild type and the mutant strains were 89.25 eggs and 28.42 eggs at normal temperature, 26.77 eggs and 0.95 at high temperature, and 10.57 eggs and 1.54 at low temperature, respectively. The m_x curve describes the start times and duration of the reproductive phase. The maximal daily oviposition rate of the wild-type strain and the mutant strain occurred at 11th d and 14th d at normal temperature, 12th d and 13th d at high temperature, and 55th d and 62nd d at low temperature (Figure 5ii).

3.8. Response to extreme temperature

The survival rate of adults of the wild and mutant strains decreased with increasing stress time when exposed at 42°C. Compared to the wild strain, survival of female adults of the mutant strain was significantly lower at 30 min ($t=4.899$, $df=6$,

$P=0.003$), 60 min ($Z=-2.352$, $P=0.019$), 90 min ($t=3.911$, $df=6$, $P=0.008$), 120 min ($Z=-2.366$, $P=0.018$) and 150 min ($Z=-2.477$, $P=0.013$), while survival rate of male adults of the mutant strain was significantly lower at 30 min ($Z=-2.233$, $P=0.026$), 90 min ($t=5.217$, $df=6$, $P=0.002$), 120 min ($Z=-2.097$, $P=0.036$) and 150 min ($Z=-2.477$, $P=0.013$) (Figure 6).

3.9. Supercooling point and freezing point

The supercooling point and freezing point of mutant strain pupae were $-19.00^{\circ}\text{C} \pm 0.58^{\circ}\text{C}$ and $-7.22^{\circ}\text{C} \pm 0.39^{\circ}\text{C}$ respectively, both significantly higher than the supercooling point of $-22.74^{\circ}\text{C} \pm 0.33^{\circ}\text{C}$ ($Z=-4.529$, $P<0.001$) and freezing point of $-10.21^{\circ}\text{C} \pm 0.56^{\circ}\text{C}$ ($t=-4.366$, $df=58$, $P<0.001$) of wild strain.

4. Discussion

Insects can develop strong stress responses to climate change due to the short life cycle and high population variability in space and time (Bale et al., 2002). The ability of insects (especially at low latitudes) to respond to extreme temperatures can be critical for climate change adaptation (Misof et al., 2014). We used the CRISPR/Cas9 system to knock out *PxHacd2*, the gene involved in the synthesis of VLCFAs. We found that the deletion of *PxHacd2* affected the content of VLCFAs and the water retention capacity of the epidermis, which reduced the ability of the moth to respond to extreme temperatures, especially in terms of population dynamics.

Hacd2 from different lepidopteran insects had similar amino acid sequences and could have similar functions. The software predicted that the secondary structure of *PxHacd2* mainly contained helix and coil. *PxHacd2* had 6 transmembrane domains

and belonged to transmembrane protein (Hallgren et al., 2022).

PxHacd2 was highly expressed in the pupal stage of the moth, and the content of VLCFAs of the pupae of *P. xylostella* was also more abundant in the 4th instar larvae, and male and female adults than any other stage. These results suggested that *P. xylostella* might require more VLCFAs to maintain pupal development. We found that *PxHacd2* was highly expressed in the fat body and epidermis of the 4th instar larvae. Wicker-Thomas et al. (Wicker-Thomas et al., 2015) report that the synthesis of VLCFAs in *Drosophila* only occurs in oenocytes. The oenocyte contains much smooth endoplasmic reticulum and expresses a large number of lipid synthases, catabolic enzymes, and other lipid metabolism-related proteins (Jackson and Locke, 1989; Martins et al., 2011; Parvy et al., 2012; Qiu et al., 2012). The oenocyte is usually attached to the epidermis or scattered between fat body cells (Martins and Ramalho-Ortigao, 2012). The oenocyte may be associated with both the fat body and the epidermis.

In addition to the fat body, *PxHacd2* was also found to be expressed in other organs such as the head, Malpighian tube, silk gland, and midgut of the 4th instar larvae. This could indicate that *PxHacd2* had additional functions besides VLCFAs synthesis, such as being involved in the composition of insect cell lipids and playing an important role in cell proliferation (Zuo et al., 2018).

In this study, we found decreased expression of the *PxHacd2* gene in the 3rd instar larvae after 2 h of stress in high or low temperature environments. The function of VLCFAs in stress resistance has been widely reported, especially in plants

(Zhukov and Shumskaya, 2020). When the halophyte plant, *Suaeda altissima* (L.), is grown in 750 mM NaCl salt solution, the content of VLCFAs increases 13-fold in the above-ground organs and 4-fold in the roots compared to a ratio above-ground to root of 2.5 fold at 250 mM NaCl (optimal concentration) (Tsydendambaev et al., 2013). Plants grown in colder temperatures have a higher content of trienoic fatty acids. The silencing of transgenic tobacco plants *FAD7* ω -3 desaturase gene results in a lower trienoic fatty acid level and can adapt better to higher temperatures than normal plants (Murakami et al., 2000).

To study the role of *PxHacd2* in the response to temperature extremes in the moth, we constructed *PxHacd2*-MU via the CRISPR/Cas9 system. VLCFAs decreased significantly in the different developmental stages of the *PxHacd2* mutant strain. Dehydration of very-long-chain (3R)-3-hydroxy acyl-CoA to form very-long-chain trans-2,3-dehydroacyl-CoA was blocked after the knockout of *PxHacd2*. However, we still found VLCFAs in the mutant strain, and this could be due to the presence of other *Hacd* genes in *P. xylostella*. For example, in mice with the *Hacd1-4* genes, *Hacd1* and *Hacd2* function redundantly in extending VLCFAs (Sawai et al., 2017). Both *Hacd1* and *Hacd2* are also found in the fruit fly *Drosophila melanogaster* and mosquito *Aedes aegypti* (Holze et al., 2021; Matthews et al., 2016). We found *PxHacd3* (XM_011552725.3) in the *P. xylostella* genome-sequencing databases in addition to *PxHacd2*. *PxHacd2* and *PxHacd3* could be functionally redundant in *P. xylostella*. However, even if other *Hacd* genes were present, we hypothesized that they could not completely replace the *PxHacd2* function. The absence of *PxHacd2*

still reduced the content of VLCFAs in the moths.

The VLCFAs are not only important precursors of hydrocarbon (major components of epidermal lipids) but also directly involved in the synthesis of the epidermis (Cerkowniak et al., 2013; Sutton et al., 2013). We found that *PxHacd2* knockout reduced the contents of VLCFAs in *P. xylostella*, which lowered the content of lipids involved in epidermis formation. This caused increased epidermal permeability of *P. xylostella*. The loss of water through cuticular transpiration accounts for more than 90% of total water loss in most terrestrial arthropods studied to date (Gibbs, 2002). The water retention capacity of insects is mainly derived from their epidermal lipids (Sutton et al., 2013; Teerawanichpan et al., 2010), especially long-chain lipids (Gibbs et al., 2005). Reduced epidermal lipid content increases epidermal permeability, which makes it easier for water molecules to pass through the insect epidermis (Locke, 1963). The RNA interference knockout of *LmFAS1* and *LmFAS3* in the locust, *Locusta migratoria* also leads to a reduction in the content of certain components of epidermal lipids and causes enhanced epidermal permeability (Yang et al., 2020).

We also found that male and female adults of the mutant strain were significantly less able to survive in different humidity environments compared to the wild strain. Increased epidermal permeability increased transpiration in *P. xylostella*, disrupting the water balance and reducing its ability to survive under both drought conditions and normal humidity (Liu et al., 2022). The survival rate of the mutant strain was higher in high humidity than normal humidity, but was still lower than the

survival rate of the wild strain at high humidity.

Extreme heat and drought often co-occur. Elevated temperatures can amplify the severity of drought by enhancing moisture evaporation, and drought also favors atmospheric warming, creating conditions for extreme heat or heat waves (Dai, 2013). The reduced number of days of survival of the mutant strain when exposed to drought stress treatment indicated that *PxHacd2* affected the drought resistance of *P. xylostella*. The results suggested that altered epidermal permeability due to reduced levels of VLCFAs might be the main reason for the reduction in the number of days of survival of the moth at different humidity levels. Some studies have found that RNA interferes with the *NIELOs2, 3, and 8* in of fatty acid synthesis pathway of the brown rice planthopper, *Nilaparvata lugens*, or the *LmFAS1, LmFAS3, and LmELO7* of *L. migratoria* causes a reduction in the content of CHCs (Li et al., 2019; Yang et al., 2020; Zhao et al., 2020). These changes can reduce their ability to survive under low humidity and normal humidity.

We calculated the life tables of each strain at different temperatures. The r (high: -0.16 ± 0.06 ; low: -0.05 ± 0.01), R_0 (high: 0.10 ± 0.06 ; low: 0.03 ± 0.02), and λ (high: 0.85 ± 0.05 ; low: 0.94 ± 0.01) of mutant strain at both high and low temperatures showed that knocking out *PxHacd2* reduced life history parameters of *P. xylostella* that are key to its capacity to maintain its population size. This indicated that *PxHacd2* might play a key role in temperature adaptability. The development and reproduction of *PxHacd2*-MU at normal temperature were also affected. This was most likely due to altering epidermal permeability caused by *PxHacd2* knockout. In

insects, fatty acids have important functions in development, metamorphosis, and reproduction. For example, Alabaster et al. (2011) used RNAi to reduce the expression of the acetyl coenzyme A carboxylase (*ACC*) and fatty acid synthase 1 (*FAS1*) genes in *Aedes aegypti*, leading to reduced lipid biosynthesis (14C-triacylglycerol, 14C-phospholipid, etc.) and lower fecundity.

Here, the *PxHacd2*-MU had a reduced ability to respond to temperature extremes. The involvement of insect epidermal lipids in maintaining water balance in vivo has been reported (Prange, 1996). When the ambient temperature exceeds the critical transition temperature, the lipid starts to liquify (Gibbs, 2002), leading to increased epidermal permeability and water loss (Chown et al., 2011; Rourke and Gibbs, 1999). At 33°C, the cockroach epidermal lipids may undergo a "phase change", resulting in a more or less sudden increase in transpiration water loss from the epidermis (Ramsay, 1935). Wigglesworth reports this phenomenon in many insects. In most of these insects, the temperature at which the "phase change" occurs is much higher than the lethal temperature (Wigglesworth, 1945). Our results also showed that the "phase transition" temperature was reduced in both male and female *PxHacd2*-MU adults. The mutant strain might have lost more water through transpiration than the wild strain, reducing its longevity. Interestingly, we found a significant increase in both the freezing point and supercooling point of *PxHacd2*-MU pupae. Fatty acids are involved in the composition of phospholipids, which are major components of the membrane's bilayer structure. The fluidity and stability of biofilms are closely related to cold resistance (Upchurch, 2008). A higher content of

unsaturated fatty acids is associated with higher membrane fluidity (Miquel et al., 1993; Wang et al., 2019). Previous reports have found that VLCFAs promote plant resistance to low temperatures by increasing their unsaturation (Zhukov and Shumskaya, 2020). Total VLCFAs contents were significantly decreased in the *PxHacd2*-MU, reducing the conversion of unsaturated VLCFAs at low temperatures. These results might be a reason for the increase in supercooling point and freezing point.

In this study, we demonstrated that *PxHacd2* knockout reduced the content of VLCFAs in *P. xylostella*, which affected the moth's epidermal permeability and reduced its water retention capacity. These findings are consistent with previous reports in plants. These changes ultimately affected the development and reproduction of *P. xylostella* at different temperatures and its ability to respond to temperature extremes. Therefore we think that *PxHacd2* can be used as a molecular drug candidate target for *P. xylostella* control in the context of global climate change. *PxHacd2* knockout did not eliminate the VLCFAs, and *PxHacd3* may have the same or similar functionality as *PxHacd2*. Studies to knock out both *PxHacd2* and *PxHacd3* are further needed in *P. xylostella*. It should also be mentioned that it remains to be determined whether *PxHacd2* has other functions, as *PxHacd2* was also expressed in tissues other than fat bodies and the epidermis. Considering the involvement of VLCFAs in plant resistance to diverse environmental stressors such as pathogens, salt, heavy metals (Zhukov and Shumskaya, 2020), the same function in insects needs to be further investigated.

Data availability

The data that support the findings of this study are available on request from the corresponding author upon reasonable request.

Acknowledgements

This research was funded by the Natural Science Foundation for Distinguished Young Scholars of Fujian Province (2022J06013), Fujian Science and Technology Project (2022L3087), the National Natural Science Foundation of China (No. 31972271, 32202312), the Fujian Agriculture and Forestry University Science and Technology Innovation Fund Project (CXZX2019001G, CXZX2017206), and the Outstanding Young Scientific Research Talents Program of Fujian Agriculture and Forestry University (xjq201905).

References

- Alabaster, A., Isoe, J., Zhou, G., Lee, A., Murphy, A., Day, W.A., Miesfeld, R.L., 2011. Deficiencies in acetyl-CoA carboxylase and fatty acid synthase 1 differentially affect eggshell formation and blood meal digestion in *Aedes aegypti*. *Insect Biochem. Mol. Biol.* 41, 946-955.
- Bach, L., Michaelson, L.V., Haslam, R., Bellec, Y., Gissot, L., Marion, J., Da Costa, M., Boutin, J.P., Miquel, M., Tellier, F., 2008. The very-long-chain hydroxy fatty acyl-CoA dehydratase PASTICCINO2 is essential and limiting for plant development. *Proc. Natl. Acad. Sci. U.S.A.* 105, 14727-14731.
- Balabanidou, V., Grigoraki, L., Vontas, J., 2018. Insect cuticle: a critical determinant of insecticide resistance. *Curr. Opin. Insect. Sci.* 27, 68-74.
- Bale, J.S., Masters, G.J., Hodkinson, I.D., Awmack, C., Bezemer, T.M., Brown, V.K., Butterfield, J., Buse, A., Coulson, J.C., Farrar, J., 2002. Herbivory in global climate change research: direct effects of

- rising temperature on insect herbivores. *Glob Chang Biol* 8, 1-16.
- Bauerfeind, S.S., Fischer, K., 2014. Simulating climate change: temperature extremes but not means diminish performance in a widespread butterfly. *Popul Ecol.* 56, 239-250.
- Bazinet, A.L., Marshall, K.E., MacMillan, H.A., Williams, C.M., Sinclair, B.J., 2010. Rapid changes in desiccation resistance in *Drosophila melanogaster* are facilitated by changes in cuticular permeability. *J. Insect Physiol.* 56, 2006-2012.
- Beament, J., 1958. The effect of temperature on the water-proofing mechanism of an insect. *J. Exp. Biol.* 35, 494-519.
- Beani, L., Bagnères, A.G., Elia, M., Petrocelli, I., Cappa, F., Lorenzi, M.C., 2019. Cuticular hydrocarbons as cues of sex and health condition in *Polistes dominula* wasps. *Insectes Soc* 66, 543-553.
- Beyenbach, K.W., 2016. The plasticity of extracellular fluid homeostasis in insects. *J. Exp. Biol.* 219, 2596-2607.
- Blomquist, G.J., Ginzl, M.D., 2021. Chemical ecology, biochemistry, and molecular biology of insect hydrocarbons. *Annu. Rev. Entomol.* 66, 45-60.
- Cassagne, C., Lessire, R., Pechouire, J., Moreau, P., Creach, A., Schneider, F., Sturbois, B., 1994. Biosynthesis of very long chain fatty acids in higher plants. *Prog. Lipid Res.* 33, 55-69.
- Cerkowniak, M., Puckowski, A., Stepnowski, P., Gołębowski, M., 2013. The use of chromatographic techniques for the separation and the identification of insect lipids. *J. Chromatogr. B.* 937, 67-78.
- Chen, N., Fan, Y. L., Bai, Y., Li, X. D., Zhang, Z. F., Liu, T. X., 2016. Cytochrome P450 gene, *CYP4G51*, modulates hydrocarbon production in the pea aphid, *Acyrtosiphon pisum*. *Insect Biochem. Mol. Biol.* 76, 84-94.

- Chen, Y., Liu, Z., Régnière, J., Vasseur, L., Lin, J., Huang, S., Ke, F., Chen, S., Li, J., Huang, J., 2021. Large-scale genome-wide study reveals climate adaptive variability in a cosmopolitan pest. *Nat. Commun.* 12, 1-11.
- Chi, H., 1988. Life-table analysis incorporating both sexes and variable development rates among individuals. *Environ. Entomol.* 17, 26-34.
- Chown, S.L., Sørensen, J.G., Terblanche, J.S., 2011. Water loss in insects: an environmental change perspective. *J. Insect Physiol.* 57, 1070-1084.
- Chung, H., Carroll, S.B., 2015. Wax, sex and the origin of species: dual roles of insect cuticular hydrocarbons in adaptation and mating. *Bioessay* 37, 822-830.
- Conley-LaComb, M.K., Saliganan, A., Kandagatla, P., Chen, Y.Q., Cher, M.L., Chinni, S.R., 2013. PTEN loss mediated Akt activation promotes prostate tumor growth and metastasis via CXCL12/CXCR4 signaling. *Mol. Cancer* 12, 85.
- Dai, A., 2013. Increasing drought under global warming in observations and models. *Nat Clim Chang* 3, 52-58.
- Danielsen, E.T., Moeller, M.E., Yamamoto, N., Ou, Q., Laursen, J.M., Soenderholm, C., Zhuo, R., Phelps, B., Tang, K., Zeng, J., Kondo, S., Nielsen, C.H., Harvald, E.B., Faergeman, N.J., Haley, M.J., O'Connor, K.A., King-Jones, K., O'Connor, M.B., Rewitz, K.F., 2016. A *Drosophila* genome-wide screen identifies regulators of steroid hormone production and developmental timing. *Dev. Cell* 37, 558-570.
- Ebrahimi, M., Sahragard, A., Talaei-Hassanloui, R., Kavousi, A., Chi, H., 2013. The life table and parasitism rate of *Diadegma insulare* (Hymenoptera: Ichneumonidae) reared on larvae of *Plutella xylostella* (Lepidoptera: Plutellidae), with special reference to the variable sex ratio of

- the offspring and comparison of jackknife and bootstrap techniques. *Ann. Entomol. Soc. Am.* 106, 279-287.
- Engvall, E., Perlmann, P., 1971. Enzyme-linked immunosorbent assay (ELISA). Quantitative assay of immunoglobulin G. *Immunochem* 8, 871-874.
- Furlong, M.J., Wright, D.J., Dossall, L.M., 2013. Diamondback moth ecology and management: problems, progress, and prospects. *Annu. Rev. Entomol* 58, 517-541.
- Gibbs, A.G., 2002. Lipid melting and cuticular permeability: new insights into an old problem. *J. Insect Physiol.* 48, 391-400.
- Gibbs, A.G., 2011. Thermodynamics of cuticular transpiration. *J. Insect Physiol.* 57, 1066-1069.
- Gibbs, A.G., Fukuzato, F., Matzkin, L.M., 2003. Evolution of water conservation mechanisms in *Drosophila*. *J. Exp. Biol.* 206, 1183-1192.
- Gibbs, A.G., Rajpurohit, S., 2010. Cuticular lipids and water balance. *Insect Hydrocarb. Biol. Biochem. Chem. Ecol.* 100-120.
- Ginzel, M.D., Blomquist, G.J. 2010. Insect hydrocarbons: biochemistry and chemical ecology, In: *Extracellular composite matrices in arthropods*. Springer, pp. 221-252.
- Gołębiowski, M., Maliński, E., Nawrot, J., Stepnowski, P., 2008. Identification and characterization of surface lipid components of the dried-bean beetle *Acanthoscelides obtectus* (Say)(Coleoptera: Bruchidae). *J Stored Prod Res.* 44, 386-388.
- Hallgren, J., Tsirigos, K.D., Pedersen, M.D., Armenteros, J.J.A., Marcatili, P., Nielsen, H., Krogh, A., Winther, O., 2022. DeepTMHMM predicts alpha and beta transmembrane proteins using deep neural networks. *bioRxiv*.
- Hao, S.G., Kang, L., 2004. Supercooling capacity and cold hardiness of the eggs of the grasshopper

- Chorthippus fallax* (Orthoptera: Acrididae). Eur. J. Entomol. 101, 231-236.
- Holze, H., Schrader, L., Buellesbach, J., 2021. Advances in deciphering the genetic basis of insect cuticular hydrocarbon biosynthesis and variation. Heredity (Edinb) 126, 219-234.
- Howard, R.W., Blomquist, G.J., 2005. Ecological, behavioral, and biochemical aspects of insect hydrocarbons. Annu. Rev. Entomol. 50, 371-393.
- Huang, Y., Wang, Y., Zeng, B., Liu, Z., Xu, X., Meng, Q., Huang, Y., Yang, G., Vasseur, L., Gurr, G.M., You, M., 2017. Functional characterization of Pol III U6 promoters for gene knockdown and knockout in *Plutella xylostella*. Insect Biochem. Mol. Biol. 89, 71-78.
- Hwang, W.Y., Fu, Y., Reyon, D., Maeder, M.L., Tsai, S.Q., Sander, J.D., Peterson, R.T., Yeh, J., Joung, J.K., 2013. Efficient genome editing in zebrafish using a CRISPR-Cas system. Nat. Biotechnol. 31, 227-229.
- Jackson, A., Locke, M., 1989. The formation of plasma membrane reticular systems in the oenocytes of an insect. Tissue Cell 21, 463-473.
- Ji, T., Guo, Y., Kim, K., McQueen, J., Ghaffar, S., Christ, A., Lin, C., Eskander, R., Zi, X., Hoang, B.H., 2015. Neuropilin-2 expression is inhibited by secreted Wnt antagonists and its down-regulation is associated with reduced tumor growth and metastasis in osteosarcoma. Mol. Cancer 14, 86.
- Jiang, M., Wang, Z., Xia, F., Wen, Z., Chen, R., Zhu, D., Wang, M., Zhuge, X., Dai, J., 2022. Reductions in bacterial viability stimulate the production of Extra-intestinal Pathogenic Escherichia coli (ExPEC) cytoplasm-carrying Extracellular Vesicles (EVs). PLoS Pathog. 18, e1010908.
- Kang, L., Chen, B., Wei, J. N., Liu, T. X., 2009. Roles of thermal adaptation and chemical ecology in *Liriomyza* distribution and control. Annu. Rev. Entomol. 54, 127-145.
- Krupp, J.J., Nayal, K., Wong, A., Millar, J.G., Levine, J.D., 2020. Desiccation resistance is an adaptive

- life-history trait dependent upon cuticular hydrocarbons, and influenced by mating status and temperature in *D. melanogaster*. *J. Insect Physiol.* 121, 103990.
- Li, D. T., Chen, X., Wang, X. Q., Moussian, B., Zhang, C. X., 2019. The fatty acid elongase gene family in the brown planthopper, *Nilaparvata lugens*. *Insect Biochem. Mol. Biol.* 108, 32-43.
- Li, J., Dai, C., Xie, W., Zhang, H., Huang, X., Chronis, C., Ye, Y., Zhang, W., 2022. A One-step strategy to target essential factors with auxin-inducible degron system in mouse embryonic stem cells. *Front. Cell Dev. Biol.* 10, 964119.
- Liu, X.J., Li, J., Sun, Y.W., Liang, X.Y., Zhang, R., Zhao, X.M., Zhang, A., Zhang, J.Z., 2022. A nuclear receptor *HR4* is essential for the formation of epidermal cuticle in the migratory locust, *Locusta migratoria*. *Insect Biochem. Mol. Biol.* 143, 103740.
- Locke, M., 1965. Permeability of insect cuticle to water and lipids. *Science* 147, 295-298.
- Martins, G., Ramalho-Ortigao, J., 2012. Oenocytes in insects. *Invertebr. Surviv. J.* 9, 139-152.
- Martins, G.F., Ramalho-Ortigão, J.M., Lolo, J.F., Severson, D.W., McDowell, M.A., Pimenta, P.F.P., 2011. Insights into the transcriptome of oenocytes from *Aedes aegypti* pupae. *Mem. Inst. Oswaldo Cruz* 106, 308-315.
- Matthews, B.J., McBride, C.S., DeGennaro, M., Despo, O., VossHall, L.B., 2016. The neurotranscriptome of the *Aedes aegypti* mosquito. *BMC Genom.* 17, 1-20.
- Miquel, M., James Jr, D., Dooner, H., Browse, J., 1993. Arabidopsis requires polyunsaturated lipids for low-temperature survival. *Proc. Natl. Acad. Sci. U.S.A.* 90, 6208-6212.
- Misof, B., Liu, S., Meusemann, K., Peters, R.S., Donath, A., Mayer, C., Frandsen, P.B., Ware, J., Flouri, T., Beutel, R.G., 2014. Phylogenomics resolves the timing and pattern of insect evolution. *Science* 346, 763-767.

- Murakami, Y., Tsuyama, M., Kobayashi, Y., Kodama, H., Iba, K., 2000. Trienoic fatty acids and plant tolerance of high temperature. *Science* 287, 476-479.
- Neven, L.G., 2000. Physiological responses of insects to heat. *Postharvest Biol. Technol.* 21, 103-111.
- Parvy, J.P., Napal, L., Rubin, T., Poidevin, M., Perrin, L., Wicker-Thomas, C., Montagne, J., 2012. *Drosophila melanogaster* Acetyl-CoA-carboxylase sustains a fatty acid-dependent remote signal to waterproof the respiratory system. *PLoS Genet.* 8, e1002925.
- Pettitt, T.R., Jones, A.L., Harwood, J.L., 1989. Lipids of the marine red alga, *Chondrus crispus* and *Polysiphonia lanosa*. *Phytochemistry.* 28, 399-405.
- Popov, V., Antipina, O., Pchelkin, V., Tsydendambaev, V., 2012. Changes in the content and composition of lipid fatty acids in tobacco leaves and roots at low-temperature hardening. *Russ. J. Plant Physiol.* 59, 177-182.
- Prange, H.D., 1996. Evaporative cooling in insects. *J. Insect Physiol.* 42, 493-499.
- Qiu, Y., Tittiger, C., Wicker-Thomas, C., Le Gruff, G., Young, S., Wajnberg, E., Fricaux, T., Taquet, N., Blomquist, G.J., Feyereisen, R., 2012. An insect-specific P450 oxidative decarboxylase for cuticular hydrocarbon biosynthesis. *Proc. Natl. Acad. Sci. U.S.A.* 109, 14858-14863.
- Ramsay, J., 1935. The evaporation of water from the cockroach. *J. Exp. Biol.* 12, 373-383.
- Roelofs, D., Janssens, T.K., Timmermans, M.J., Nota, B., Marien, J., Bochdanovits, Z., Ylstra, B., Van Straalen, N.M., 2009. Adaptive differences in gene expression associated with heavy metal tolerance in the soil arthropod *Orchesella cincta*. *Mol. Ecol.* 18, 3227-3239.
- Rourke, B.C., Gibbs, A.G., 1999. Effects of lipid phase transitions on cuticular permeability: model membrane and in situ studies. *J. Exp. Biol.* 202, 3255-3262.
- Sawai, M., Uchida, Y., Ohno, Y., Miyamoto, M., Nishioka, C., Itohara, S., Sassa, T., Kihara, A., 2017. The

- 3-hydroxyacyl-CoA dehydratases *HACD1* and *HACD2* exhibit functional redundancy and are active in a wide range of fatty acid elongation pathways. *J. Biol. Chem.* 292, 15538-15551.
- Sutton, P.A., Wilde, M.J., Martin, S.J., Cvačka, J., Vrkoslav, V., Rowland, S.J., 2013. Studies of long chain lipids in insects by high temperature gas chromatography and high temperature gas chromatography–mass spectrometry. *J. Chromatogr. A.* 1297, 236-240.
- Talekar, N., Shelton, A., 1993. Biology, ecology, and management of the diamondback moth. *Annu. Rev. Entomol.* 38, 275-301.
- Teerawanichpan, P., Robertson, A.J., Qiu, X., 2010. A fatty acyl-CoA reductase highly expressed in the head of honey bee (*Apis mellifera*) involves biosynthesis of a wide range of aliphatic fatty alcohols. *Insect Biochem. Mol. Biol.* 40, 641-647.
- Tsydendambaev, V., Ivanova, T., Khalilova, L., Kurkova, E., Myasoedov, N., Balnokin, Y.V., 2013. Fatty acid composition of lipids in vegetative organs of the halophyte *Suaeda altissima* under different levels of salinity. *Russ. J. Plant Physiol.* 60, 661-671.
- Tvrđik, P., Westerberg, R., Silve, S., Asadi, A., Jakobsson, A., Cannon, B., Loison, G., Jacobsson, A., 2000. Role of a new mammalian gene family in the biosynthesis of very long chain fatty acids and sphingolipids. *J. Cell Biol.* 149, 707-718.
- Upchurch, R.G., 2008. Fatty acid unsaturation, mobilization, and regulation in the response of plants to stress. *Biotechnol. Lett.* 30, 967-977.
- van Wilgenburg, E., Sulc, R., Shea, K.J., Tsutsui, N.D., 2010. Deciphering the chemical basis of nestmate recognition. *J. Chem. Ecol.* 36, 751-758.
- Vincent, J.F., 2001. *Encyclopedia of materials: science and technology*. Elsevier. pp. 1924-1928.
- Vincent, J.F., Wegst, U.G., 2004. Design and mechanical properties of insect cuticle. *Arthropod Struct*

- Dev 33, 187-199.
- Wang, X., Yu, C., Liu, Y., Yang, L., Li, Y., Yao, W., Cai, Y., Yan, X., Li, S., Cai, Y., 2019. GmFAD3A, a ω -3 fatty acid desaturase gene, enhances cold tolerance and seed germination rate under low temperature in rice. *Int. J. Mol. Sci.* 20, 3796.
- Wang, Y., Yu, Z., Zhang, J., Moussian, B., 2016. Regionalization of surface lipids in insects. *Proc. Royal Soc. B.* 283, 20152994.
- Wicker-Thomas, C., Garrido, D., Bontonou, G., Napal, L., Mazuras, N., Denis, S., Rubin, T., Parvy, J.-P., Montagne, J., 2015. Flexible origin of hydrocarbon/pheromone precursors in *Drosophila melanogaster*. *J. Lipid Res.* 56, 2094-2101.
- Wigglesworth, V., 1945. Transpiration through the cuticle of insects. *J. Exp. Biol.* 21, 97-114.
- Wigglesworth, V., 1970. Structural lipids in the insect cuticle and the function of the oenocytes. *Tissue Cell* 2, 155-179.
- Xie, C., Xiong, L., Ye, M., Shen, L., Li, J., Zhang, Z., You, M., You, S., 2022. Genome-wide analysis of *V-ATPase* genes in *Plutella xylostella* (L.) and the potential role of *PxVHA-G1* in resistance to *Bacillus thuringiensis* Cry1Ac toxin. *Int. J. Biol. Macromol.* 194, 74-83.
- Xie, J., Ge, W., Li, N., Liu, C., Chen, F., Yang, X., Huang, X., Ouyang, Z., Zhang, Q., Zhao, Y., Liu, Z., Gou, S., Wu, H., Lai, C., Fan, N., Jin, Q., Shi, H., Liang, Y., Lan, T., Quan, L., Li, X., Wang, K., Lai, L., 2019. Efficient base editing for multiple genes and loci in pigs using base editors. *Nat. Commun.* 10, 2852.
- Xie, S., Du, Y., Zhang, Y., Wang, Z., Zhang, D., He, L., Qiu, L., Jiang, J., Tan, W., 2020. Aptamer-based optical manipulation of protein subcellular localization in cells. *Nat. Commun.* 11, 1347.
- Xu, Y., Wu, C., Cao, X., Gu, C., Liu, H., Jiang, M., Wang, X., Yuan, Q., Wu, K., Liu, J., Wang, D., He, X.,

- Wang, X., Deng, S.J., Xu, H.E., Yin, W., 2022. Structural and biochemical mechanism for increased infectivity and immune evasion of Omicron BA.2 variant compared to BA.1 and their possible mouse origins. *Cell Res.* 32, 609-620.
- Yang, F.Y., Chen, J.H., Ruan, Q.Q., Wang, B.B., Jiao, L., Qiao, Q.X., He, W.Y., You, M.S., 2021. Fitness comparison of *Plutella xylostella* on original and marginal hosts using age-stage, two-sex life tables. *Ecol. Evol.* 11, 9765-9775.
- Yang, Y., Zhao, X., Niu, N., Zhao, Y., Liu, W., Moussian, B., Zhang, J., 2020. Two fatty acid synthase genes from the integument contribute to cuticular hydrocarbon biosynthesis and cuticle permeability in *Locusta migratoria*. *Insect Mol. Biol.* 29, 555-568.
- Yeh, P.Y., Lu, Y.S., Ou, D.L., Cheng, A.L., 2011. IkappaB kinases increase Myc protein stability and enhance progression of breast cancer cells. *Mol. Cancer* 10, 53.
- You, M., Ke, F., You, S., Wu, Z., Liu, Q., He, W., Baxter, S.W., Yuchi, Z., Vasseur, L., Gurr, G.M., 2020. Variation among 532 genomes unveils the origin and evolutionary history of a global insect herbivore. *Nat. Commun.* 11, 1-8.
- Zhao, X., Yang, Y., Niu, N., Zhao, Y., Liu, W., Ma, E., Moussian, B., Zhang, J., 2020. The fatty acid elongase gene *Lm Elo7* is required for hydrocarbon biosynthesis and cuticle permeability in the migratory locust, *Locusta migratoria*. *J. Insect Physiol.* 123, 104052.
- Zhou, H., Lei, G., Chen, Y., You, M., You, S., 2022. *PxTret1-like* affects the temperature adaptability of a cosmopolitan pest by altering trehalose tissue distribution. *Int. J. Mol. Sci.* 23.
- Zhou, Y., Zeng, L., Fu, X., Mei, X., Cheng, S., Liao, Y., Deng, R., Xu, X., Jiang, Y., Duan, X., Baldermann, S., Yang, Z., 2016. The sphingolipid biosynthetic enzyme *Sphingolipid delta8* desaturase is important for chilling resistance of tomato. *Sci. Rep.* 6, 38742.

Zhukov, A.V., Shumskaya, M., 2020. Very-long-chain fatty acids (VLCFAs) in plant response to stress.

Funct. Plant Biol. 47, 695-703.

Zou, M.M., Wang, Q., Chu, L.N., Vasseur, L., Zhai, Y.L., Qin, Y.D., He, W.Y., Yang, G., Zhou, Y.Y., Peng, L.,

You, M.S., 2020. CRISPR/Cas9-induced vitellogenin knockout lead to incomplete embryonic

development in *Plutella xylostella*. Insect Biochem. Mol. Biol. 123, 103406.

Zuo, W., Li, C., Luan, Y., Zhang, H., Tong, X., Han, M., Gao, R., Hu, H., Song, J., Dai, F., 2018.

Genome-wide identification and analysis of elongase of very long chain fatty acid genes in

the silkworm, *Bombyx mori*. Genome 61, 167-176.

Journal Pre-proof

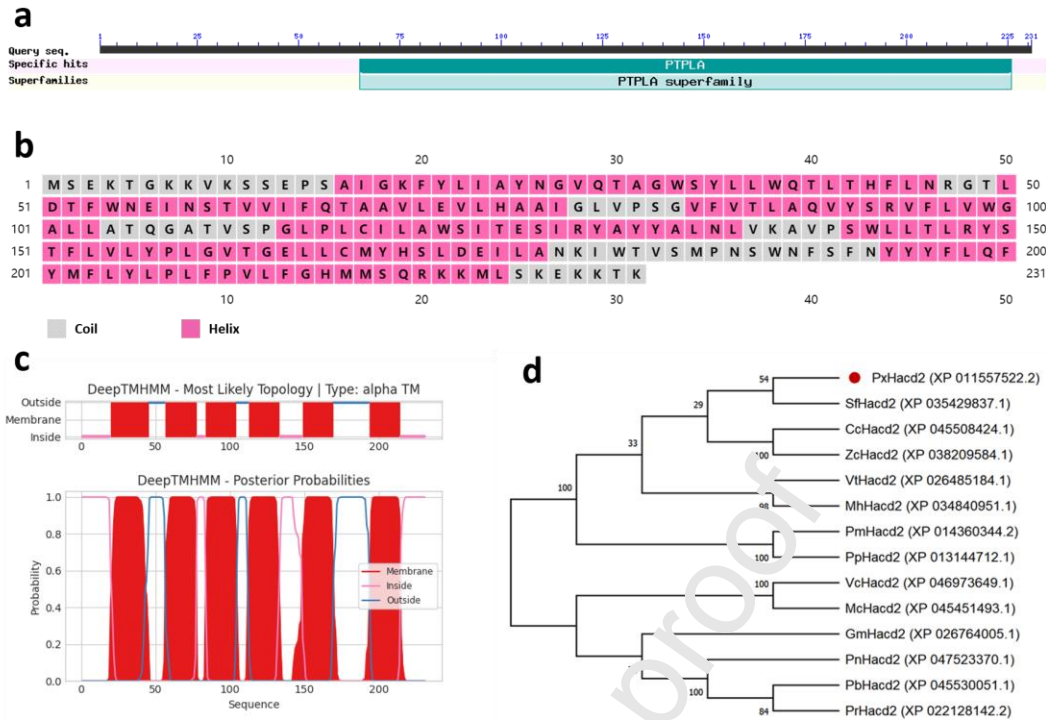


Figure 1. Characterization of *P. xylostella* *PxHacd2* gene. (a) The conserved domain of *PxHacd2*.

(b) Secondary structure of *PxHacd2*. Grey represents coil; pink represents helix. (c) The

transmembrane domain of *PxHacd2*. The red line represents a membrane; the pink line represents the inside of the protein and the blue line, the outside. (d) Phylogenetic tree of

PxHacd2 from different insects based on amino acid sequences. *PxHacd2* is marked by a red dot.

P. xylostella: *PxHacd2*; *Stenopora frugiperda*: *SfHacd2*; *Colias croceus*: *CcHacd2*; *Zerene cesonia*:

ZcHacd2; *Vanessa tamamea*: *VtHacd2*; *Maniola hyperantus*: *MhHacd2*; *Papilio machaon*:

PmHacd2; *Papilio polyte*: *PpHacd2*; *Vanessa cardui*: *VcHacd2*; *Melitaea cinxia*: *McHacd2*; *Galleria*

mellonella: *GmHacd2*; *Pieris napi*: *PnHacd2*; *Pieris brassicae*: *PbHacd2*; *Pieris rapae*: *PrHacd2*.

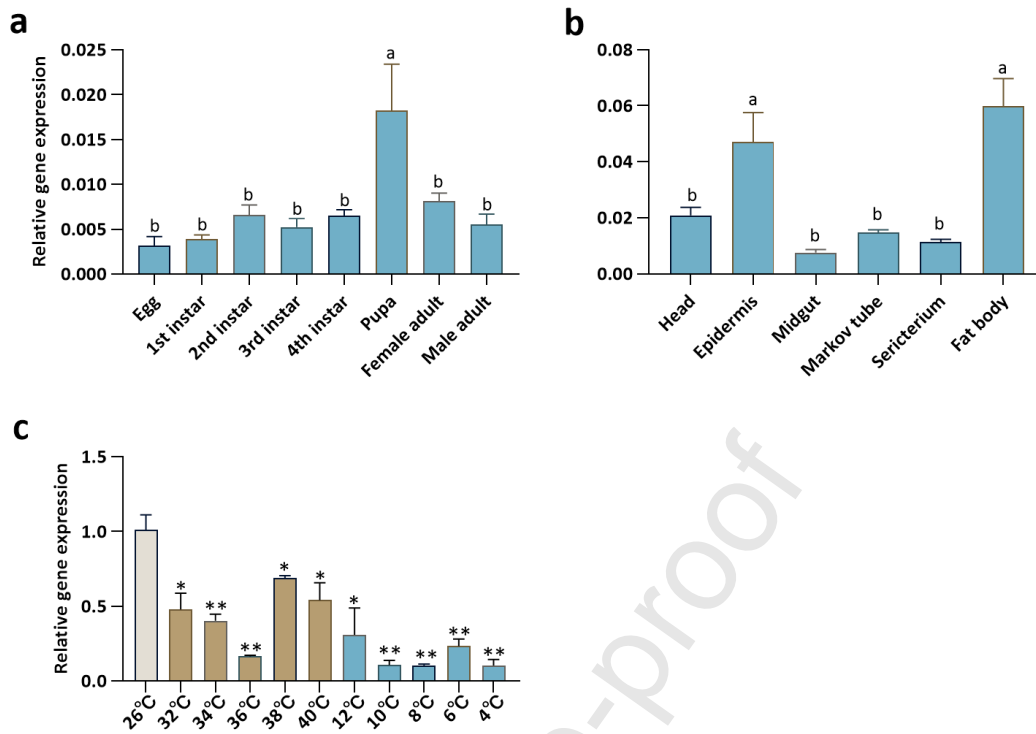


Figure 2. The expression patterns of *PxHacd2* in *P. xylostella*. (a) Expression of *PxHacd2* at different stages. (b) Expression of *PxHacd2* in different tissues of the 4th instar larvae. (c) Expression of *PxHacd2* in 3rd instar larvae stressed for 2 h at high (32°C, 34°C, 36°C, 38°C, 40°C) and low (12°C, 10°C, 8°C, 6°C, 4°C) temperatures. The Student–Newman–Keuls test was used to analyze the expression of *PxHacd2* at different developmental stages and tissues. Different letters indicate significant differences ($P < 0.05$) in relative expression levels. The independent-sample t-tests were performed to compare the expression levels of the *PxHacd2* gene of 3rd instar larvae between those treated for 2 hours of high and low temperature stress and those at 26°C. Asterisk (*) indicates $P < 0.05$; (**) indicates $P < 0.01$.

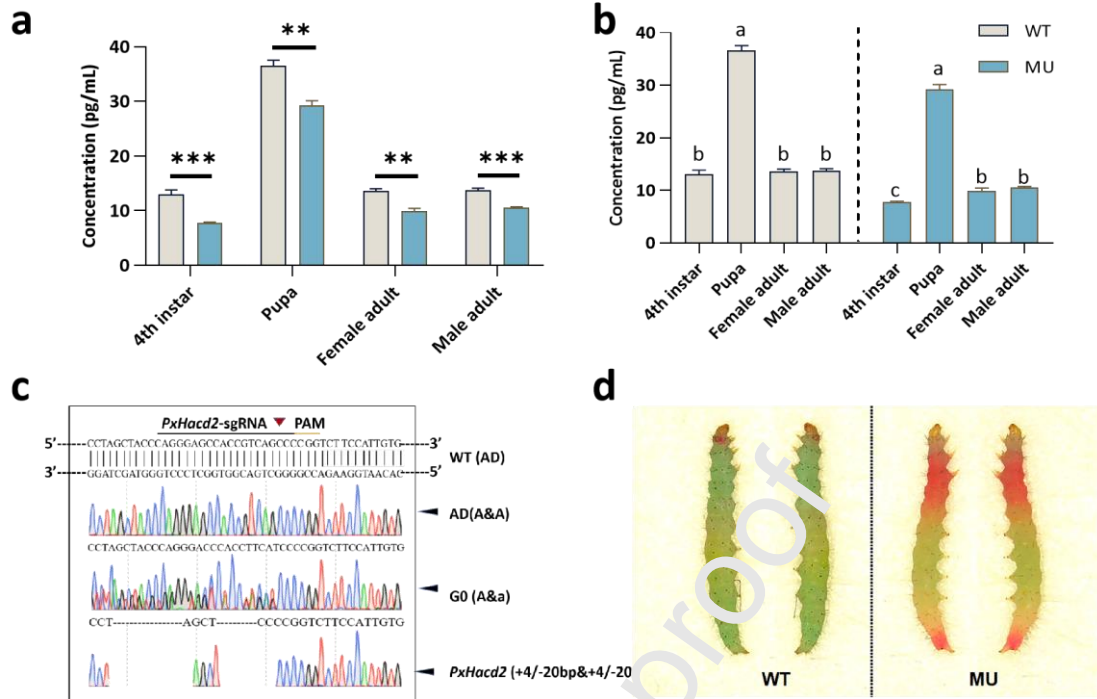


Figure 3. (a) Comparison of *PxHacd2*-Mutant (MU) and wild type (WT), VLCFAs content was significantly reduced in the mutant strain. Independent-sample t-test was used. Asterisk (**) indicates $P < 0.01$; (***) indicates $P < 0.001$. (b) Comparison of *PxHacd2*-Mutant (MU) and wild type (WT), VLCFAs content was highest in pupae. The Student-Newman-Keuls test was used and different letters indicate significant differences in VLCFAs content. (c) Targeted mutation of *P. xylostella PxHacd2* mediated by CRISPR/Cas9. The sgRNA target sequence of *PxHacd2* was identified in exon 3 and is underlined; the PAM sequence adjacent to the sgRNA target sequence is also underlined, and the cleavage site is indicated with a red inverted triangle. A stretch of typical multiple peaks of PCR products directing sequencing was the main characteristic of mutated G0 individuals. Deleted bases are shown as dashes. (d) *PxHacd2*-Mutant (MU) and wild type (WT) strains of 4th instar larvae were stained with Eosin Y. Compared to the wild strain, the mutant strain had an impaired surface barrier against Eosin Y penetration.

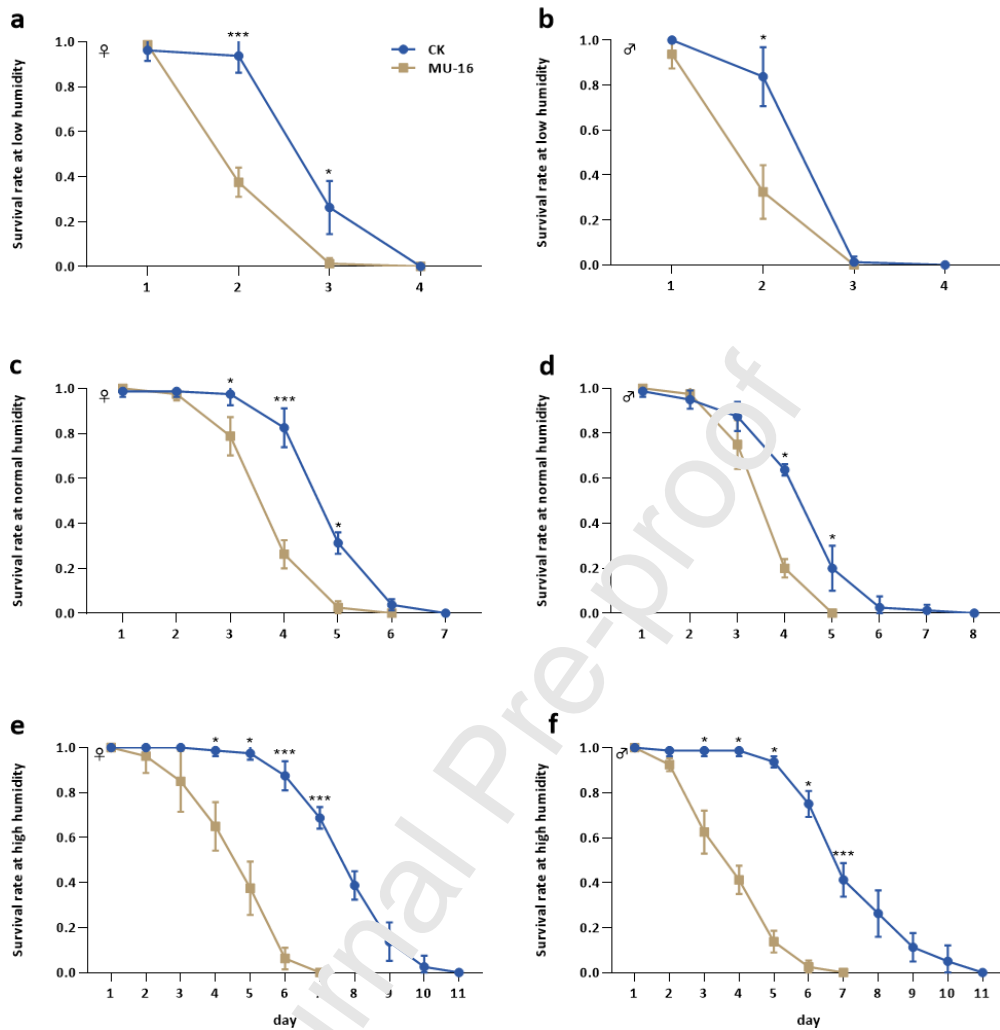


Figure 4. Effect of knocking out *PxHacd2* on the survival rate of adults in different humidity environments. (a, b) Low humidity treatments (<10%); (c, d) Normal humidity treatments (60±5%); (e, f) High humidity treatments (>90%). The viability of both male and female adults in different humidity environments was decreased compared with that of the wild-type strain. Error bars represent the standard error of the mean. Data represent 20 female adults or male adults per repetition and each replication was repeated 4 times. Asterisk (*) indicates $P < 0.05$; (***) indicates $P < 0.001$.

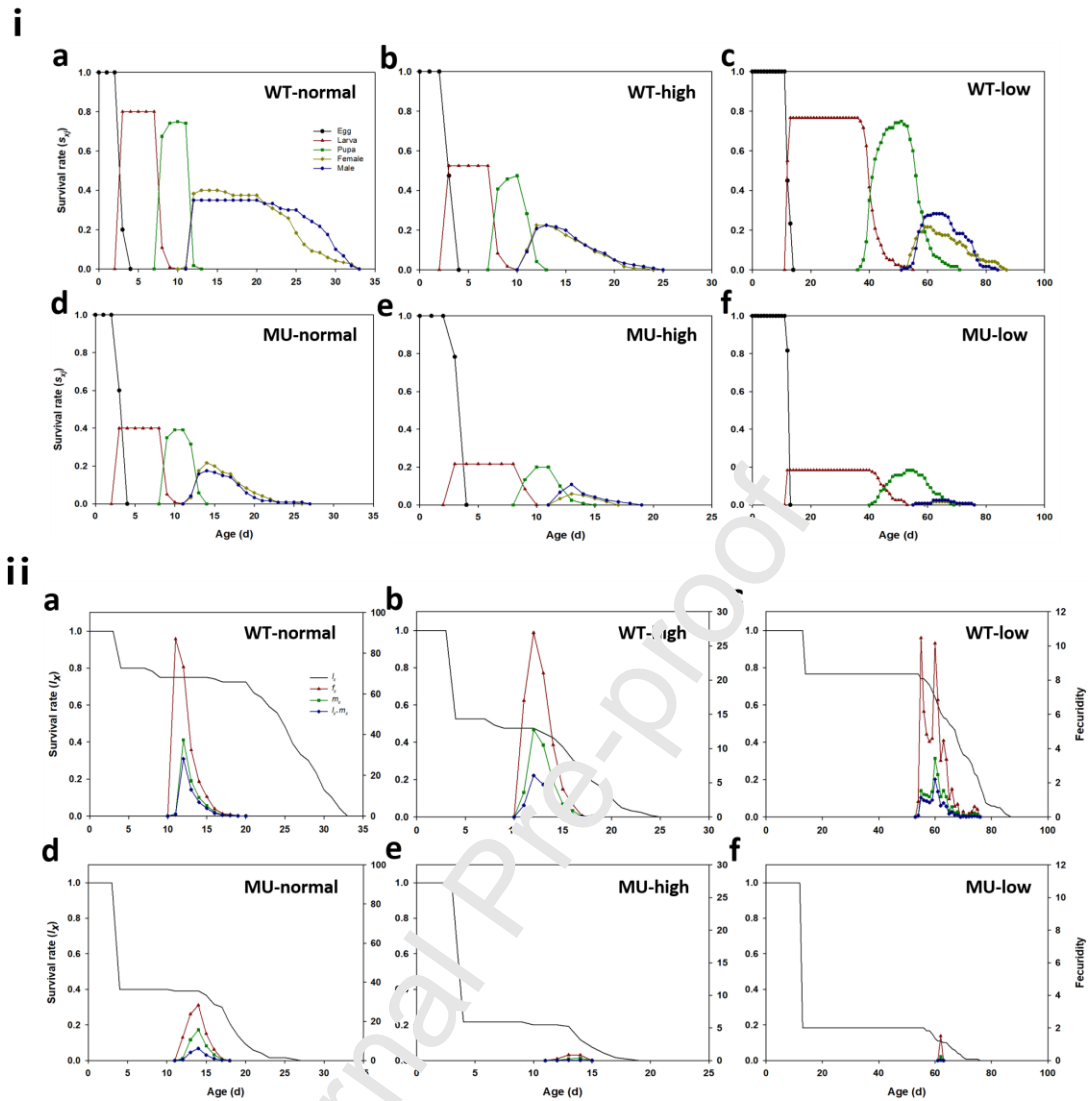


Figure 5. Age-stage survival rates (S_{xj}) (i), age-specific survival rates (l_x) (ii), female age-stage specific fecundity (j_x) (ii) and age-specific fecundity of total population (m_x) (ii) of wild and mutant strains of *P. xylostella* at different temperature environments. The survival rate of immature stage of the mutant strain was lower than that of the wild strain at different temperatures.

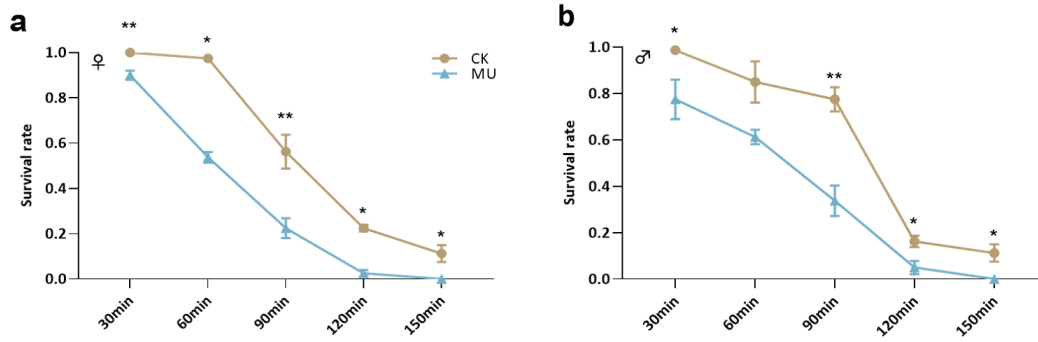


Figure 6. Effects of *PxHacd2* knockout on the survival of adults exposed to extreme temperatures at different times. Mutant strain was less resistant to extreme heat compared to wild strain, and mutant strain couldn't survive to 150 min compared to the wild strain. Asterisk (*) indicates $P < 0.05$; (**) indicates $P < 0.01$. Data represent 20 female adults or male adults per repetition and each replication was repeated 4 times.

Table 1 Primers used in this study

Primer	Primer sequence (5'-3')
<i>PxHacd2</i> -CDS-F	ATGTCTGAGAAAACCGCAAG
<i>PxHacd2</i> -CDS-R	CAACTCGTTTCTCTTTTCTGTTTCATT
Q- <i>PxHacd2</i> -F	ACCGCAAGAAAGTGAAGAGT
Q- <i>PxHacd2</i> -R	AGTGCCAGAGTTCCACGGTT
Q- <i>PxRPL32</i> -F	CAATCAGGCCAATTTACCGC
Q- <i>PxRPL32</i> -R	CTGCGTTTACGCCAGTACG
<i>PxHacd2</i> -SgRNA-F ^a	<u>TAATACGACTCACTATAGGCAGGG</u> <u>TGCACCGTCAGCCCG</u>
	TTTTAGAGCTAGAAATAGCTAGTTAAAATAAGGCTAGTCC
sgRNA-Com-R ^b	AAAAGCACCGACTCGGTGCCTACTTTTCAAGTTGATAAC
	GGACTAGCCTTATTAACTTGCTATTTCTAGCTCTAAAA
<i>PxHacd2</i> -F	CTGCATGCAGCTATTGGC
<i>PxHacd2</i> -R	TCTACCTAACTGCTGATTCATATCATAC

Note: ^a T7 promoter sequence is a single underline. The target site is double underline. ^b It is a universal reverse primer.

Table 2 Developmental time, longevity, Adult preoviposition period (APOP), Total preoviposition period (TPOP), fecundity, oviposition and population parameters on mutants and wild-type strain at different temperature environments.

Parameter	Normal temperature		High temperature		Low temperature	
	WT	<i>PxHacd2-MU</i>	WT	<i>PxHacd2-MU</i>	WT	<i>PxHacd2-MU</i>
Egg (d)	3.00±0.00	3.00±0.00	3.00±0.00	3.00±0.00	12.28±0.05	12.00±0.00*
Larva (d)	5.11±0.04	6.11±0.05*	5.18±0.06	6.33±0.13*	29.49±0.33	34.18±0.72*
Pupa (d)	3.90±0.04	3.85±0.10	3.51±0.07	3.33±0.12	15.97±0.13	16.60±0.60
Adult Female (d)	13.27±0.57	5.96±0.56*	5.83±0.50	2.88±0.52*	17.56±1.61	9.50±0.50*
Adult Male (d)	16.60±0.49	6.24±0.53*	6.85±0.51	2.44±0.42*	16.31±0.81	11.33±2.67
Adult All (d)	14.82±0.42	6.09±0.38*	6.12±0.36	2.58±0.32*	16.85±0.83	10.60±1.54*
Longevity All (d)	21.36±0.93	9.95±0.69*	10.87±0.65	6.35±0.42*	56.52±2.25	22.43±1.84*
APOP (d)	0.00±0.00	0.28±0.11*	0.04±0.04	0.67±0.33	1.82±0.36	2.00±0.00
TPOP (d)	11.98±0.02	13.32±0.14*	11.70±0.13	13.00±0.58*	56.59±0.39	62.00±0.00*
Oviposition (d)	4.93±0.24	2.64±0.24*	3.65±0.29	1.00±0.00*	7.41±0.69	1.00±0.00*
Fecundity (eggs)	151.9±7.70	69.52±8.13*	81.78±9.39	1.50±0.89*	63.23±10.06	3.00±0.00*
r (d ⁻¹)	0.29±0.01	0.18±0.01*	0.20±0.02	-0.16±0.06*	0.04±0.01	-0.06±0.01*
R_0 (eggs/female)	54.43±7.19	14.48±3.07*	15.68±3.44	0.10±0.06*	11.59±2.87	0.03±0.02*
T (d)	13.68±0.05	14.93±0.14*	13.57±0.13	14.36±0.52	60.69±0.47	63.00±0.00*
λ (d ⁻¹)	1.34±0.01	1.20±0.02*	1.22±0.02	0.85±0.05*	1.04±0.01	0.94±0.01*

Note: The intrinsic rate of increase (r), net reproductive rate (R_0), finite rate of increase (λ), and generation time (T). The data of treatments were compared by using the paired bootstrap test.

Values are means \pm standard errors; Asterisk (*) indicates $P < 0.05$ difference between mutant and the wild-type strain.

Journal Pre-proof

CRedit authorship contribution statement

All the authors read and approved the final version of the manuscript. Details of each author with their contribution in this paper are shown as below:

Gaoke Lei: Methodology; Writing-original draft preparation; Data curation; Formal analysis.

Huiling Zhou: Methodology; Investigation; Data curation.

Yanting Chen: Methodology; Writing-review and editing.

Liette Vasseur: Conceptualization; Writing-review and editing; Formal analysis.

Geoff M. Gurr: Reviewed manuscript for significant intellectual content and scholarly contribution to interpretation of results; Supervision.

Minsheng You: Conceptualization; Writing-review and editing; Funding acquisition; Supervision.

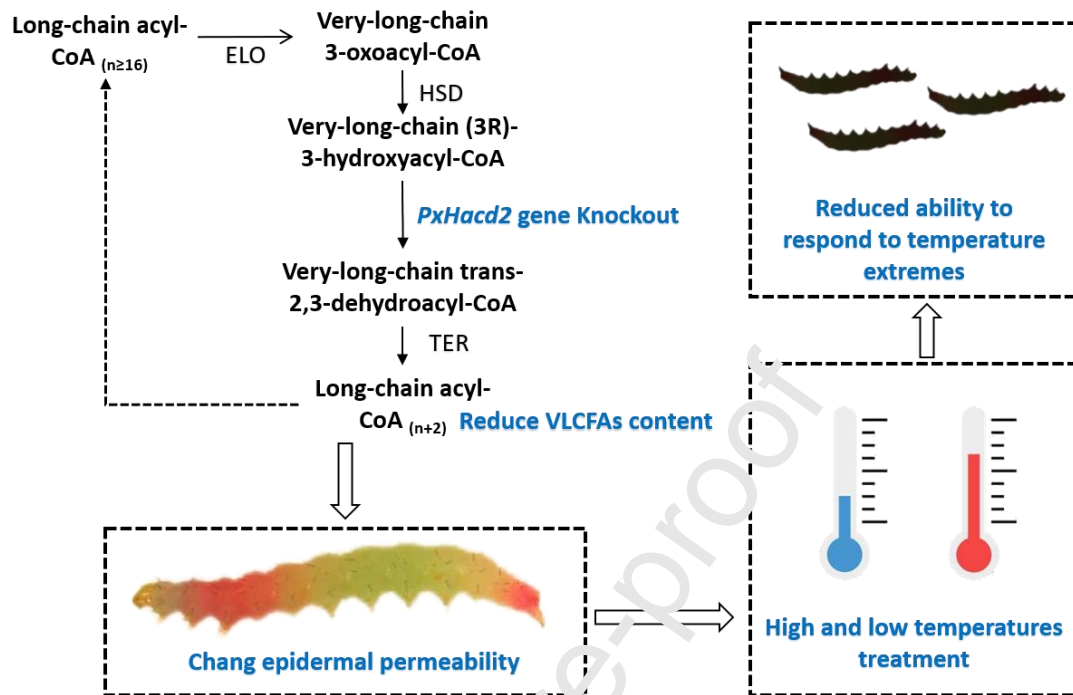
Shijun You: Conceptualization; Writing-review and editing; Supervision; Funding acquisition; Project administration.

Declaration of interest statement

The authors declare that they have no known competing financial interests or personal relationships that could have appeared to influence the work reported in this paper.

Journal Pre-proof

Graphical abstract



Highlights

- Differential expression of the *PxHacd2* gene in the moth at different temperatures.
- Very long-chain fatty acid (VLCFA) decreased in *PxHacd2*-deficient strain.
- Epidermal permeability increased with the decreased VLCFAs.
- Pest's temperature adaptability affected by effects on epidermal permeability.

Journal Pre-proof